Journal of Engineering Physics and Thermophysics, Vol. 65, No. 3, 1993

USE OF TVD-SCHEMES TO SIMULATE GASDYNAMIC FLOWS WITH SPHERICAL AND CYLINDRICAL SYMMETRY

I. M. Kozlov, G. S. Romanov, and
A. E. Suvorov

UDC 519.6

A generalization of the Harten TVD-scheme in the form of a predictor-corrector-type scheme of second-order accuracy in time and space is proposed for the flows with spherical and cylindrical symmetry. The scheme does not require introducing components with artificial viscosity and describes discontinuities in the solution without the appearance of nonphysical oscillations for a Courant number less than 0.8.

The concept of a TVD-scheme (a scheme with a reduction in the total variation) has been introduced by Harten [1]. It can be shown that for the scalar conservation law

$$\frac{\partial U}{\partial t}+\frac{\partial F(U)}{\partial x}=0 \tag{1}$$

the total variation

$$TV=\int\left|\frac{\partial U}{\partial x}\right|dx \tag{2}$$

is conserved if the solution is smooth, and decreases when discontinuities are present. According to this, a scheme has the TVD property if numerical analog of (2)

$$TV=\Sigma|U_{j+1}-U_j| \tag{3}$$

does not increase at each step. It is evident that this property provides not only scheme stability, but prevents development of nonphysical numerical oscillations.

For gas dynamics equations, U and F are vectors: $U=\begin{bmatrix}\rho\\ \rho v\\ e\end{bmatrix}$, $F=\begin{bmatrix}\rho v\\ \rho v^2\\ (e+p)v\end{bmatrix}$. In this case the total variation for a system of nonlinear conservation laws (1), generally speaking, can also increase, for example, during interaction between shock waves. Therefore there are no reasons to call for always satisfying the TVD condition in the scheme. The generalization of the scalar TVD-schemes to the case of systems of nonlinear hyperbolic equations is performed via the expansion of U_{j+1}-U_j in eigenvectors of the matrix $\partial F/\partial U$ and the use of the scalar TVD-scheme for each expansion component, which is a variant of solving the linearized Riemann problem [2]. Here the TVD condition and, along with it, the absence of oscillations occur when calculating noninteracting waves. For interacting waves, good quality of the solution is in no way theoretically substantiated but is verified by a large number of computations. Having restricted ourselves to consideration of explicit schemes, we may say that the calculation of the change in the quantity U at each step in time is performed using flows defined at the boundaries of the cells by the formula

$$F_{j+1/2}=\frac{1}{2}(F_j+F_{j+1}+R_{j+1/2}\Phi_{j+1/2}). \tag{4}$$

Academic Scientific Complex "A. V. Luikov Heat and Mass Transfer Institute of the Academy of Sciences of Belarus," Minsk. Translated from Inzhenerno-Fizicheskii Zhurnal, Vol. 65, No. 3, pp. 296-301, September, 1993. Original article submitted June 15, 1992.

1062-0125/93/6503-0861$12.50

Here $R_{j+1/2}$ is the matrix of eigenvectors of $\partial F/\partial U$, which is determined from any symmetric average of U_{j+1} and U_j. Various expressions for the vector $\Phi_{j+1/2}$ are given in [3, 4]. The first two components in (4) correspond to the usual scheme in central differences of first order in t and second order in x, whereas the last component provides second order in time and numerical dissipation, suppressing the nonphysical oscillations typical of traditional central-difference schemes.

Direct generalization of (4) to spherical or cylindrical geometries of the problem is impossible, because in this case the gas dynamics equations

$$\frac{\partial \rho}{\partial t}+\frac{1}{r^\lambda}\frac{\partial}{\partial r}(r^\lambda \rho v)=0,\quad \frac{\partial}{\partial t}(\rho v)+\frac{1}{r^\lambda}\frac{\partial}{\partial r}(r^\lambda \rho v^2)+\frac{\partial p}{\partial r}=0,$$
$$\frac{\partial e}{\partial t}+\frac{1}{r^\lambda}\frac{\partial}{\partial r}[r^\lambda v(e+p)]=0,\quad e=\rho\left(\varepsilon+\frac{v^2}{2}\right), \tag{5}$$
$$\lambda=\begin{cases}0-\text{plane layer}\\1-\text{cylinder}\\2-\text{sphere}\end{cases}$$

are not of the form of Eq. (1). Therefore, we should interpolate separately the pressure and convective flows at the cell boundaries. Furthermore, the TVD principle itself is not applicable here, generally speaking, even to individual waves, since a shock wave, converging to the symmetry center, is enhanced without bound [6, 7]. Because of this, to develop a scheme retaining the good qualities of plane TVD-schemes, we used a simple heuristical method that reduces to the following. It is known that traditional central-difference schemes describe well the flow everywhere, except the discontinuity region, and therefore, if to such a scheme we add numerical dissipation, typical of a plane TVD-scheme, then it is more or less obvious that this scheme will take on the good qualities of TVD-scheme if the discontinuity is located sufficiently far from the center. In the opposite case (say, during reflection of a converging shock wave) we can and must verify the efficiency of such a scheme by a numerical experiment. As the base scheme we used a predictor-corrector-type scheme:

$$\Delta\rho_j=\frac{\Delta t}{\Delta V_j}[(S\rho v)_{j-1/2}-(S\rho v)_{j+1/2}],$$
$$\Delta(\rho v)_j=\frac{\Delta t}{\Delta V_j}[(S\rho v^2)_{j-1/2}-(S\rho v^2)_{j+1/2}]+\frac{\Delta t}{\Delta r_j}(p_{j-1/2}-p_{j+1/2}),$$
$$\Delta e_j=\frac{\Delta t}{\Delta V_j}[(Sv(e+p))_{j-1/2}+(Sv(e+p))_{j+1/2}],\quad S_{j+1/2}=r^\lambda_{j+1/2}, \tag{6}$$
$$\Delta r_j=r_{j+1/2}-r_{j-1,2},\quad \Delta V_j=\frac{1}{\lambda+1}(r^{\lambda+1}_{j+1/2}-r^{\lambda+1}_{j-1/2}).$$

In formulas (6) the index j refers to the middle of a cell, and the indices $j\pm1/2$ to its boundaries. The values of ρv, ρv^2, $v(e+p)$, p at the cell boundaries are obtained by means of linear interpolation of these values at the centers of the cells. Computations by formulas (6) are performed twice, namely, once with a half step in time and the second time with the full step. Thereafter, numerical dissipation that corresponds to the TVD-scheme developed previously in [1] and modified in [3, 5] is added. For this purpose we calculate the flows by the formulas

$$f_{j+1/2}=\frac{1}{2}R_{j+1/2}\Phi_{j+1/2},$$
$$\Phi^l_{j+1/2}=\Delta r_{j+1/2}\left\{\frac{1}{2}\psi(a^l_{j+1/2})(g^l_{j+1}+g^l_j)-\psi(a^l_{j+1/2}+\gamma^l_{j+1/2})\alpha^l_{j+1/2}\right\}, \tag{7}$$
$$\Delta r_{j+1/2}=r_{j+1}-r_j,\quad \psi(Z)=\begin{cases}|Z| & |Z|\geqslant\delta,\\(Z^2+\delta^2)/2\delta & |Z|<\delta,\end{cases}$$

where a^l is an eigenvalue of $\partial F/\partial U$, $\alpha^l_{j+1/2}$ are elements of $R^{-1}_{j+1/2}(U_{j+1}-U_j)/\Delta r_{j+1/2}$, while the values

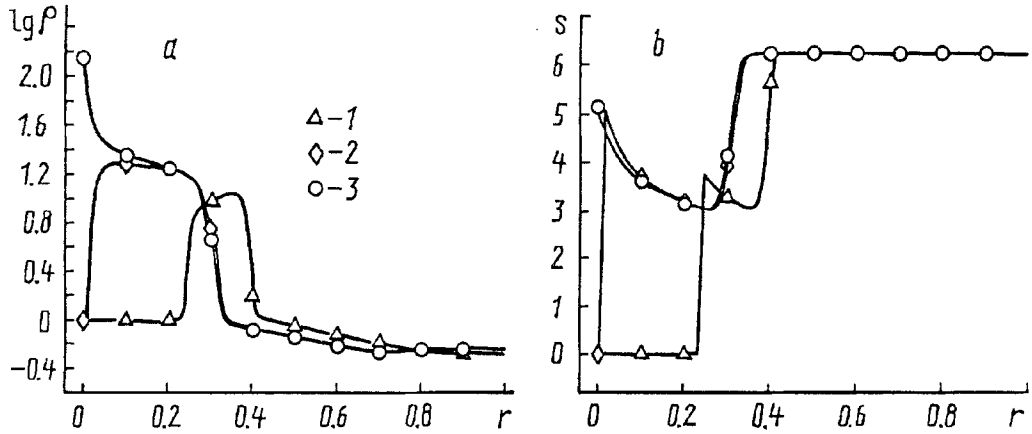

Fig. 1. Dependence of gas parameters on the radius for a converging shock wave (a - density; b - entropy, $s = \log(p/\rho^{\gamma})$): 1) $t = 2.53 \cdot 10^{-2}$; 2) $3.23 \cdot 10^{-2}$; 3) $3.29 \cdot 10^{-2}$.

$$\gamma_{j+1/2}^{l} = \frac{1}{2}\psi(a_{j+1/2}^{l}) \begin{cases} (g_{j+1}^{l} - g_{j}^{l})/\alpha_{j+1/2}^{l} & \alpha_{j+1/2}^{l} \neq 0, \\ 0 & \alpha_{j+1/2}^{l} = 0, \end{cases} \tag{8}$$

$$g_{j}^{l} = \operatorname{minmod}(\alpha_{j-1/2}^{l},\ \alpha_{j+1/2}^{l}), \tag{9}$$

$$g_{j}^{l} = I \max[0,\ \min(2|\alpha_{j+1/2}^{l}|,\ I\alpha_{j-1/2}^{l}),\ \min(|\alpha_{j+1/2}^{l}|,\ 2I\alpha_{j-1/2}^{l})],$$

$$I = \operatorname{sgn}(\alpha_{j+1/2}^{l}). \tag{9a}$$

The minmod function is equal to the least-in-magnitude argument, if all the arguments are of the same sign, or to zero, if the arguments are different in sign. Formula (9) may be used successfully in the calculations of Φ^{l} for all eigenvalues. In [3] it is indicated that if we apply (9) to the eigenvalues $v \pm c$, and (9a) to the eigenvalue v, then we may obtain the best description of the contact discontinuity. Our calculations verify this conclusion for spherical and cylindrical problems. However it should be borne in mind that, according to [3], the application of (9a) can lead in certain situations to scheme instability. The change of the gasdynamic parameters because of numerical dissipation is equal to

$$\Delta U_{j} = \frac{\Delta t}{\Delta V}[(Sf)_{j+1/2} - (Sf)_{j-1/2}]. \tag{10}$$

Let us consider in more detail the eigenvalues of the matrix

$$\frac{\partial F}{\partial U} = \begin{bmatrix} 0 & 1 & 0 \\ \chi - 0{,}5(2-k)v^2 & (2-k)v & k \\ (\chi + 0{,}5kv^2 - H)v & H - kv^2 & (1+k)v \end{bmatrix}, \tag{11}$$

where the following notation is introduced [4]: $\chi = (\partial p/\partial \rho)_{\rho\varepsilon}$, $k = (\partial p/\partial \rho\varepsilon)_{\rho}$, $H = (e + p)/\rho$. Note that for an ideal gas $\chi = 0$, $k = \gamma - 1$. The velocity of sound $c^2 = \chi + k(H - v^2/2)$.. The eigenvalues of matrix (11) are $a^1 = v - c$, $a^2 = v$, $a^3 = v + c$. The corresponding matrix of the eigenvectors equals

$$R = \begin{bmatrix} 1 & 1 & 1 \\ v - c & v & v + c \\ H - vc & v^2/2 - \chi/k & H + vc \end{bmatrix}, \tag{12}$$

and its inverse matrix is

$$R^{-1} = \begin{bmatrix} 0{,}5(b_1 + v/c) & -0{,}5(vb_2 + 1/c) & b_2/2 \\ 1 - b_1 & vb_2 & -b_2 \\ 0{,}5(b_1 - v/c) & -0{,}5(vb_2 - 1/c) & b_2/2 \end{bmatrix}, \tag{13}$$

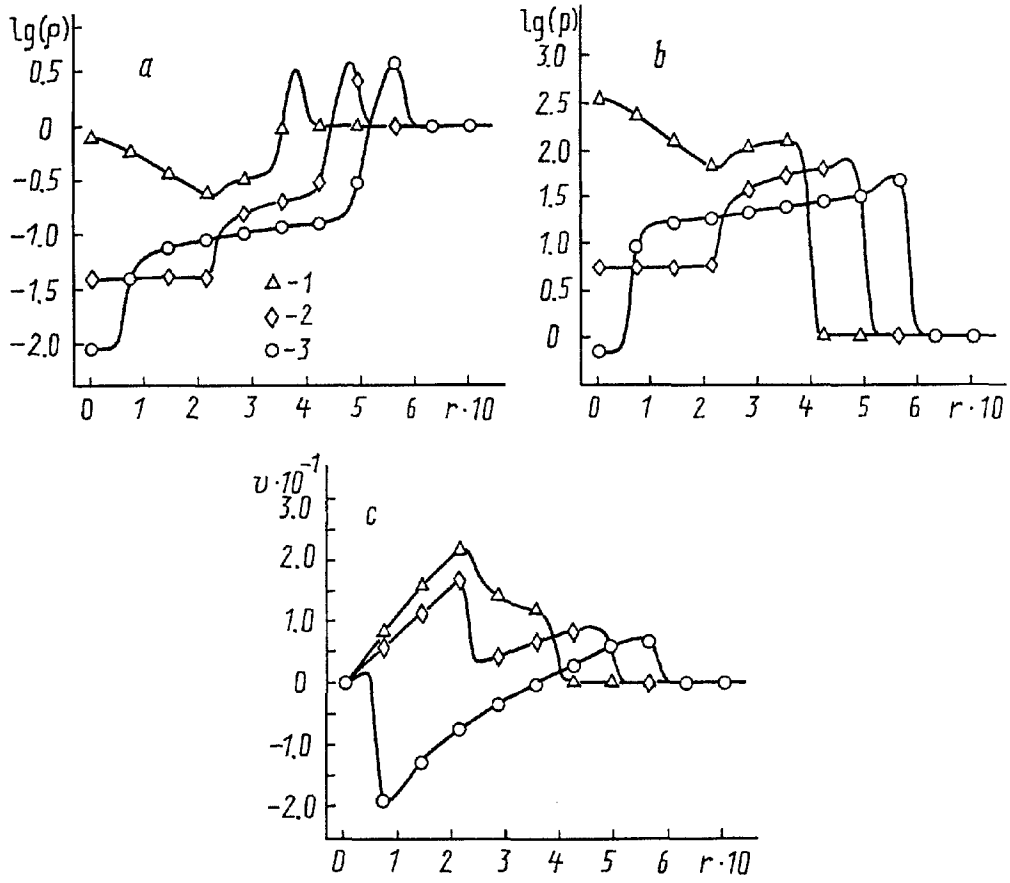

Fig. 2. Gas parameters at the initial decay stage of a spherical discontinuity, i.e., formation of a backward shock wave (a - density; b - pressure; c - velocity): 1) $t = 8.63 \cdot 10^{-3}$; 2) $1.69 \cdot 10^{-2}$, 3) $2.50 \cdot 10^{-2}$.

where $b_1 = (k\upsilon^2/2 + \chi)/c^2$, $b_2 = k/c^2$.

Since the proposed calculation scheme (6)-(10) is the least substantiated when a shock wave is located near the symmetry center, we consider the results of simulating convergence of a shock wave to the center in a spherical volume with an impermeable wall at the radius R = 1, filled by an ideal gas with $\gamma = 1.4$. At the initial instant a stagnant gas has a homogeneous density over the volume equal to 1, the pressure in the interior part of the sphere $r < 0.75$ is equal to 1, and in the section from r = 0.75 to the wall it equals 500. As a result of discontinuity decay and subsequent interaction between the rarefaction wave and the wall, a gaseous cluster is produced which moves to the sphere center. At the front of the cluster the gas is compressed sixfold in the shock wave,and then further compression of the gas caused by the spherical geometry occurs. The gaseous cluster is separated from the originally heated gas by a contact discontinuity. Figure 1a shows that for the time instant t = 0.025 the maximum compression reaches 10 and is located considerably farther from the sphere center than the shock-wave front, which is easily identified in Fig. 1b. As the shock wave moves forward, it is enhanced and the growth in entropy to the sphere center is responsible for this. For a converging shock wave there exists a self-similar solution (valid in the vicinity of the sphere center) which is substantially independent of the initial conditions [6, 7]. In particular, the maximum compression for an ideal gas with $\gamma = 1.4$ is equal to 20.1 before focusing of the shock wave at the center and reaches 145 after reflection of the shock wave. The time instant t = 0.0323 in Fig. 1 precedes the focusing, while at t = 0.0329 the density at the center reaches its greatest magnitude. The gas density agrees doubly well with the self-similar solution.

In the second case considered a heated gas with pressure equal to 500 was situated in a sphere with $r < 0.25$, while outside this sphere the pressure was equal to 1. The gas density over the whole space was equal to 1. The problem was solved in a sphere of radius R = 2. Because of discontinuity decay rather complicated motion

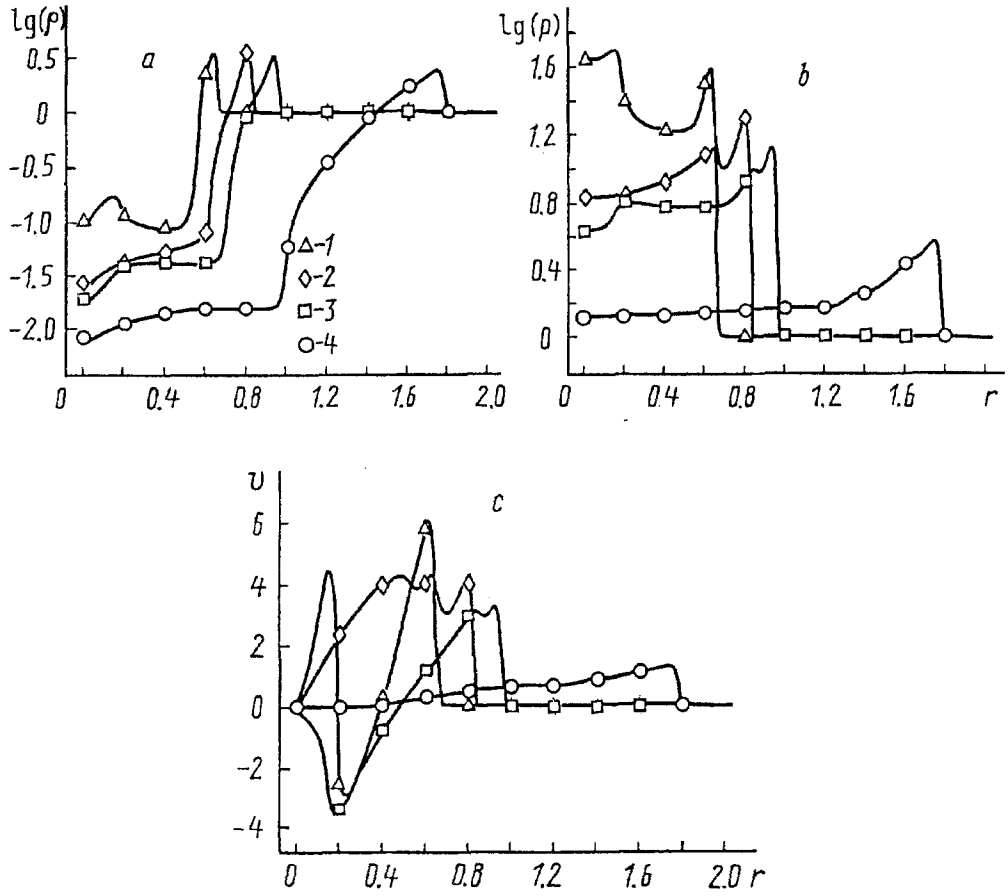

Fig. 3. Gas parameters during decay of a spherical discontinuity (a - densityl; b - pressure; c - velocity): 1) t = 3.36 $\cdot 10^{-2}$; 2) $5.93 \cdot 10^{-2}$; 3) $8.6 \cdot 10^{-2}$; 4) $3.63 \cdot 10^{-1}$.

arises. The shock wave formed carries away gas situated in the vicinity of the original pressure drop and leaves behind a quite rarefied space, to where gas located in the vicinity of the sphere center begins to flow out. The outflow velocity is found to be higher than the gas velocity behind the shock wave front. The interaction between these two flows eventually leads to the formation of another shock wave, which propagates to the sphere center. Figure 2 illustrates all stages of this process. After reflection from the center the shock wave first propagates over the rarefied hot gas (in Fig. 3a, b t = 0.0336 corresponds to this) and then collides with the contact discontinuity (t = 0.0593). As a result of the interaction with the contact discontinuity the wave is split: one part is reflected backward to the center, while the other overtakes the head shock wave (t = 0.086). Subsequently, the wave is repeatedly reflected successively from the center and from the contact discontinuity, gradually losing its energy and acquiring the character of a smooth long-wave oscillation. At t = 0.363, four wave reflections from the center had occurred. Here, the disturbance from the first reflection has already merged with the head shock wave, the next two reflections are sufficiently well seen on graphs of the pressure and velocity, and the last one is already virtually imperceptible.

All calculations were performed on a uniform grid over the radius, consisting of 200 cells. The Courant number was equal to 0.5, i.e., the step in time was determined from the relation $\Delta t = 0.5 \min (\Delta r/(c+|v|))$. Trial computations allow us to assume that the critical Courant number for the proposed method is approximately equal to 0.8. In the calculations we used formula (9) for the eigenvalues $v \pm c$ and (9a) for the eigenvalue v. To perform calculations by formulas (11)-(13), it is necessary to average v, H, k, and χ over two adjacent cells. The last two quantities are constants for an ideal gas, whereas for the first two it is recommended in the literature to use Roe averaging [2]. Our computations have shown that this technique gives no advantages in comparison with the

simplest averaging $v_{j+1/2} = (v_{j-1} + v_j)/2$ and $H_{j+1/2} = (H_{j-1} + H_j)/2$ that we have used. The quantity δ in formulas (7) was assumed to be equal to zero.

NOTATION

U, density of a conserved quantity (density, momentum, energy); F, flow; t, time; x, coordinate; ρ, density; v, velocity; e, energy density; p, pressure; R, matrix of eigenvectors; Φ, flow expansion in terms of eigenvectors; λ, curvature index; r, radius; ε, specific internal energy; Δt, step in time; ΔV, cell volume; S, area; Δr, size of a cell over the radius; f, flow through a cell boundary; H, enthalpy; c, velocity of sound; s, entropy; a, b, α, g, γ, χ, k, coefficients in equations.

REFERENCES

1. A. Harten, SIAM J. Num. Anal., **21**, 1-23 (1983).
2. P. L. Roe, J. Comp. Phys., **43**, 357-372 (1981).
3. J. Moon and H. C. Yee, AIAA Paper, No. 350, 1-17 (1987).
4. J.-L. Montagne, H. C. Yee, and H. Vinokur, AIAA J., **27**, 1332-1346 (1989).
5. H. C. Yee, International J. Comput. Math. Applications, **12A**, No. 4/5, 413-432 (1986).
6. L. D. Landau and E. M. Lifshits, Hydrodynamics [in Russian], Moscow (1986).
7. Ya. B. Zel'dovich and Yu. P. Rayzer, Physics of Shock Waves and High-Temperature Hydrodynamic Phenomena [in Russian], Moscow (1966).